14 April 2004
JLAB-TN-04-008

Estimated Beam Breakup Threshold Currents in the 10 kW FEL due to HOMs in the 7-Cell Cryomodule

C. Tennant, E. Pozdeyev, S. Simrock, A. Sun, H. Wang

Abstract

As part of the commissioning activities on the new 7-cell cryomodule for the FEL Upgrade, cold (2 K) measurements were performed to characterize the cryomodule in terms of its higher-order mode parameters (frequencies and loaded quality factors). A review of the measurement method is given. The data was then analyzed and used as inputs for the multipass, multibunch beam breakup code MATBBU to determine the threat of the instability developing at currents below those at which the FEL will operate. The results from these simulations predict that there are seven modes that produce a threshold current below 10 mA. The most offending mode is the TM110 $3\pi/7$ mode in cavity 7 which has both a large normalized R/Q (29.9 Ω) and loaded quality factor (6.11×10^6) which produces a threshold current of 2.85 mA in the vertical plane. Several schemes designed to suppress the effects of beam breakup are briefly discussed.

Introduction

This note is intended to document the higher-order mode (HOM) data from the cold measurements performed on the 7-cell cryomodule and specifically to address the implications of this data as it relates to the beam breakup (BBU) instability. Details of the BBU mechanism can be found elsewhere [1, 2]. However the underlying premise is that with insufficient damping of cavity HOMs, a positive feedback loop will be created between the cavity and the recirculated beam. This feedback can create an energy exchange between the cavity HOMs and beam which can lead to exponential beam size growth.

Cold Measurements of the 7-Cell Cryomodule

In February 2004, the third cryomodule was moved into the FEL vault. The cryomodule sits parallel to its final destination on the beamline so it can be commissioned in parallel with the FEL operation. When the cryomodule was cooled to 2 K and before the waveguides were installed, measurements of the HOM parameters were made. For each of the eight cavities, the frequencies and loaded quality-factors (Q_L) of the TM010 fundamental passband and TE111 and TM110 dipole mode passbands were measured. The details of the setup for measuring the HOM parameters are shown pictorially in Appendix A. The measurement involves using port 1 of a network analyzer to excite each cavity through the fundamental power coupler and picking up the signal through the HOM1 port with port 2 and thus completing the S21 measurement (The field probe and HOM2 ports were terminated in 50 Ω loads).

The results of the measurements on the fundamental π-mode are summarized in Table 1. During the measurement the mechanical tuners of the cavities were *not* in their operating position. This explains the ~ 200 kHz discrepancies in the fundamental π-mode frequencies from the nominal 1497 MHz. The loaded quality factors, meanwhile, show good agreement with the expected 2.0 x 10^7.

	Fundamental Freq. (MHz)	**Q_{loaded} (10^7)**
Cavity 1	1496.841	2.27
Cavity 2	1496.800	2.10
Cavity 3	1496.855	2.27
Cavity 4	1496.773	2.17
Cavity 5	1496.952	2.05
Cavity 6	1496.873	2.18
Cavity 7	1496.736	1.80
Cavity 8	1496.745	2.23

Table 1: Measured fundamental π-mode frequencies and loaded Qs of each cavity in the new FEL cryomodule (cooled to 2 K) with tuners relaxed.

Although the primary function of the mechanical tuners is to ensure the fundamental mode is at the proper resonant frequency, the tuners can also shift the HOMs. Because the BBU instability is very sensitive to the frequency of a mode, it was important to re-measure the HOM frequencies with the tuners in their operating position. With the waveguides now installed, the measurement was made by exciting the cavity through the HOM1(2) port and picking up at the HOM2(1) port. This method is sufficient to measure the frequencies of modes, however due to the significant coupling between ports ("cross-talk") the resonant curves are distorted to such an extent that an accurate loaded Q measurement is virtually impossible. (Although it would have been a good check to re-measure the loaded Q of each mode, the quality factors are not expected to change due to a change in tuner position).

A summary of the HOM data is given in the bar graphs in Appendix B. Each bar represents the shunt impedance (i.e. the product of the measured loaded quality factor and the *R/Q* given by MAFIA) for each measured frequency. The *R/Q* gives a measure of the strength of the coupling of the mode to the beam while the loaded *Q* is proportional to the time taken by a mode to dissipate the energy deposited by the beam. Therefore, those modes with a high *R/Q* and/or high Q_L pose the greatest threat for beam breakup. The data in Appendix B is in a convenient representation since dangerous modes can be recognized with only a cursory glance at the graphs.

Simulation Results

A quick review of the relevant input parameters (and the source of that information) for a given MATBBU simulation is shown below:

HOM Parameters
- Frequency (from measurements)
- Quality Factor (from measurements)
- *R/Q* (from MAFIA simulations)
- Polarization (from HOM coupler geometry)

Machine Lattice
- Elements between cryomodules (from DIMAD optics code)
- 4 x 4 transverse recirculation matrix (from DIMAD optics code)
- 4 x 4 transfer matrix through each RF cavity (from DIMAD optics code)

To date there is no measured data for HOM shunt impedances of the 7-cell cavity and so we must rely on MAFIA simulations. The results of such a simulation are shown in Table 2 where the frequencies and shunt impedances of the HOMs in the TE111 and TM110 passbands are given. The simulation calculates the *R/Q* for a 1 cm displacement off-axis and thus has units of $\{\Omega/cm^2\}$ whereas the BBU simulation programs TDBBU and MATBBU require a normalized $(R/Q)/(ka)^2$ in units of $\{\Omega\}$ [3].

To be thorough, a brief summary of results from previous MATBBU simulations (i.e. before this data was collected) is presented. As an aside, the present FEL configuration with two cryomodules (Zone 2 and Zone 4) was also simulated in TDBBU and MATBBU. Both simulations yielded a threshold current of 125 mA [4].

Frequency [MHz]	R/Q [Ω/cm^2]	$(R/Q)/(ka)^2$ [Ω]
1725.3	0.03	0.3
1746.4	0.005	0.04
1780.2	0.56	4.0
1824.0	0.37	2.5
1874.3	13.3	85.9
1926.0	10.1	61.9
1991.5	0.47	2.7
2000.6	2.93	16.7
2068.6	0.35	1.9
2089.2	5.73	29.9
2102.5	5.59	28.8
2109.7	0.28	1.4
2113.5	1.01	5.2
2113.9	0.13	0.7

Table 2: Results of MAFIA simulation for the frequencies and (*R/Q*)s of HOMs in the first two passbands in the 7-cell cavity. (The TM110 3π/7 mode is highlighted).

I. Simulations From Old HOM Measurements

It was recently discovered that an *incorrect* recirculation matrix was used in previous simulations of the FEL Upgrade with the third cryomodule installed. Although this essentially renders all previous simulation results invalid, they are presented for the sake of comparing the previously held values for the threshold current to the most recent - and accurate - values. A few words about the origin of the HOM data used in this simulation are in order. For all previous simulations of the new 7-cell cryomodule, data was combined from measurements obtained from two different sources. Warm measurements on a copper model of the 7-cell cavity were performed by H. Wang. Independently, cold measurements of a 7-cell niobium cavity in the horizontal test bed were performed by R. Campisi. The loaded quality factors of the HOMs from the measurements were then added in parallel to investigate worst case scenarios (see reference [5] for Wang's data, reference [6] for Campisi's data and reference [5] for the combined data). Those modes which were determined to have the greatest potential for causing beam breakup were simulated as being in every one of the 8 cavities in the cryomodule. Results from the simulation are shown graphically in Figure 1. The threshold current is predicted to be in the horizontal plane and expected to occur at 3.68 mA.

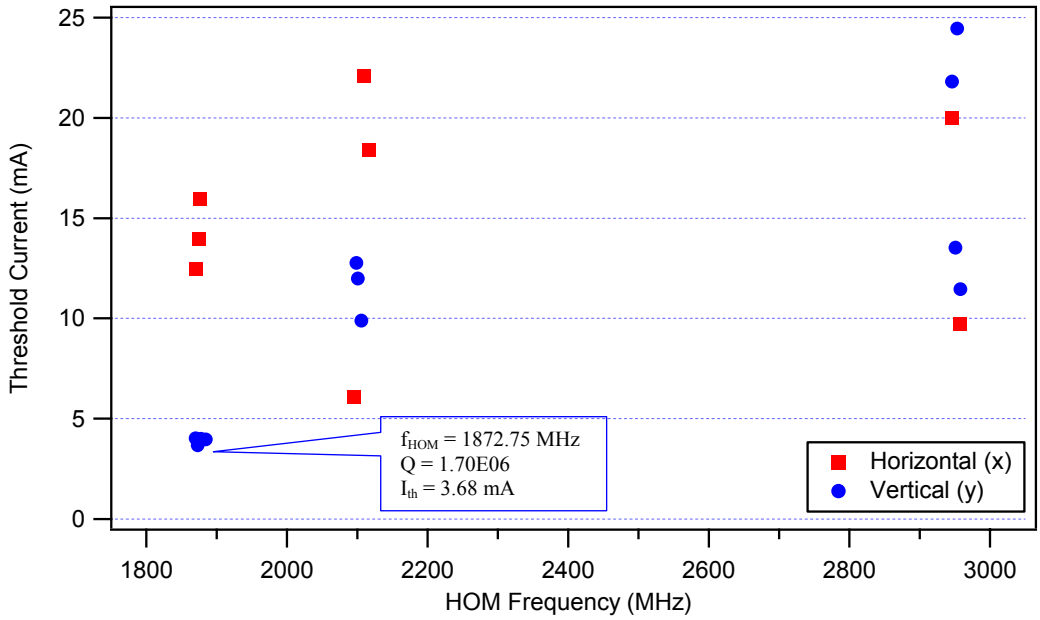

Figure 1: Simulation results from MATBBU for the threshold current in the FEL Upgrade due solely to the 7-cell cryomodule using old data with an incorrect recirculation matrix.

II. Simulations Using Data from these Cold Measurements

To avoid excessively long simulation run times, only the most dangerous HOM modes of the 7-cell cryomodule were simulated. Since the threshold current depends strongly on the product of the *R/Q* and loaded quality factor, we considered an HOM as a potential "killer-mode" candidate if $(R/Q)Q_L$ was greater than 10 $\{M\Omega/cm^2\}$ (see Appendix B). Using this criterion, the 7-cell cryomodule contains 13 HOM modes that need to be investigated. (To avoid any confusion from comparing data in Appendix B to the corresponding data found in the input file of Appendix C, note that the beam sees cavity 8 of the cryomodule *first*. Thus the first 7-cell cavity in the input file corresponds to cavity 8 in the cryomodule and so on).

Differences from previous simulations:

1. use HOM data from cold measurements
2. use correct recirculation matrix
3. include the effects of cavity focusing

One of the useful features of MATBBU is the ability for the user to explicitly define transfer matrices for each accelerating cavity. In this way, one can include cavity focusing which is known to have an appreciable effect [7]. These matrices were generated from the optics code DIMAD and are given in Appendix C.

The results of the simulation are shown in Figure 2 below and in Table 3 in the "Conclusions" section. Note that the simulation does not include HOMs higher than the third passband. Only the most dangerous modes from the first two HOM passbands were simulated. Due to time constraints we did not have the opportunity to measure the HOMs in the higher frequencies, however previous simulation results (see Figure 1) suggest that there may be some dangerous modes present at these frequencies. From our measurements, the most offending mode is the TM110 $3\pi/7$ mode in cavity 7 which produces a threshold current of 2.85 mA in the horizontal plane with a cluster of several other TM110 modes predicted to cause breakup at only slightly higher currents.

Although using data from cold measurements provides some degree of confidence in the simulation's results, there are still causes for error in the predicted threshold current. The problem comes down to a lack of adequate knowledge of all the input parameters. A short discussion of the parameters with the greatest uncertainty is given below:

1. Recirculation Transfer Matrix: The M_{12} (and M_{34}) terms describing the transport from the exit of the linac back to the entrance of the linac are based on optics simulations done before the start of FEL commissioning activities. In reality the values for the recirculation matrix will not be known until a stable orbit is established through the FEL with the 7-cell cryomodule installed.

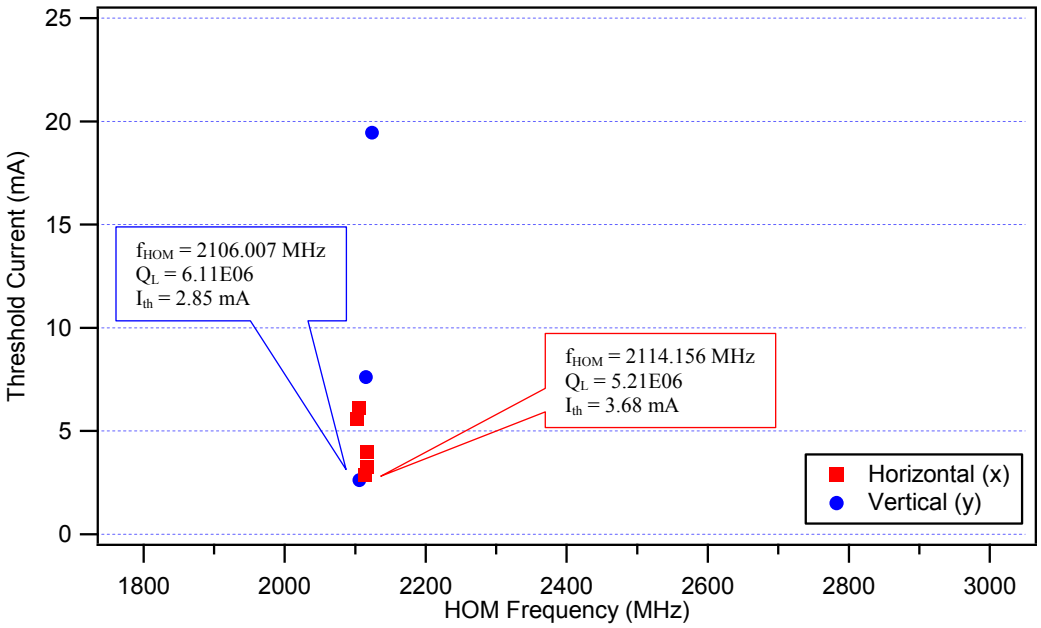

Figure 2: Simulation results from MATBBU for the threshold current in the FEL Upgrade due solely to the 7-cell cryomodule using data from cold measurements, the correct recirculation matrix and including the effects of cavity focusing.

2. HOM Polarization: On the 7-cell cavities, the HOM couplers are oriented 114 degrees apart, whereas on the 5-cell cavity, the HOM couplers are aligned with the horizontal and vertical axes of the accelerator (90 degrees apart). For the MATBBU input, an HOM is characterized by its *R/Q*, frequency, quality factor and polarization (see Table 3). The polarization can only take the values 0 or 90 degrees. Since the coupler orientation of the 7-cell cavities can not be accurately modeled, only worst case scenarios were considered. That is, each HOM included in the simulation was assigned a polarization of 0 *and* 90 degrees.

These uncertainties, in addition to the inherent errors associated with measuring the frequency and loaded Q of each mode, can cause gross over- (or under-) estimates of the predicted threshold current. Regardless, the presence of several of these dangerous modes should be a cause for concern.

Possible Cures for the Beam Breakup Instability

In order to suppress the harmful effects of beam breakup, three methods of suppressing the instability have been, and are being, investigated. The first two are valid only for a single mode per cavity, whereas the third is valid for any distribution of harmful HOMs throughout the linac:

1. Heavily Detune Cavity

As previously discussed, the threshold current is very sensitive to the frequency of the offending HOM. It is precisely because of this sensitivity that one can imagine heavily detuning the cavity that contains the dangerous HOM [8]. The detuning should be able to shift the HOM frequency on the order of a few hundred kHz, which can significantly increase the threshold current. Granted, for this method to work the cavity must be turned off, but this should be viewed as a "quick-cure" and would be effective as long as only one or two cavities contain dangerous HOMs. It would be beneficial to track the HOM frequency as a function of tuner position to see if enough frequency shift can be achieved using the tuner. This is a straightforward measurement which is planned for the near future.

2. Active HOM Damping

Another method involves actively damping the HOMs in the cavity. This is only possible in the new 7-cell cavities because of the two HOM ports in the new HOM coupler design. The idea is as follows: couple power from the HOM1 port, shift it 180 degrees in phase, put in through an amplifier and feed it through the HOM2 port (see Appendix D for details). A measurement to prove the validity of such a scheme was performed. For a specific HOM (at 1936 MHz) the loaded Q was lowered by a factor of ~ 4. If there are only a small number of dangerous modes (i.e. one per cavity), then this may be a way to lower the Q and perhaps avoid the consequences of BBU. This is a more permanent solution than the previous one, but it still is only valid for one mode per cavity.

3. Bunch-by-Bunch Feedback System

A permanent solution to combat beam breakup is in the form of a bunch-by-bunch transverse feedback system [9]. Due to the relatively short path length of the FEL, implementing a bunch-by-bunch feedback system presents both hardware and software challenges. Nevertheless, a study to investigate the effectiveness of such a system to increase the threshold current is under way. Future ERL based light sources that envision operating with ~ 100 mA of average current will certainly need a method to inhibit the onset of BBU and an active feedback system is a clear choice in accomplishing that.

Conclusions

Detailed simulations have been performed with MATBBU using recently measured data of the HOM parameters in the new 7-cell cryomodule. It is predicted that every cavity, with the exception of cavities 2 and 3, contains at least one mode which will cause beam breakup below 10 mA. All of the dangerous modes (listed in Table 3) are either $3\pi/7$ or $4\pi/7$ modes in the TM110 passband where the R/Q values are on the order of 30 Ω and where the loaded quality factors are on the order of 10^6. The combination of a

large R/Q and Q_L values conspire to produce very low threshold currents. The most dangerous mode appears to be the TM110 3π/7 mode in cavity 7, which in turn leads to a threshold current of less than 3 mA.

Several reasons why the threshold current could be different in reality were discussed. However it is clear that even if the uncertainty in the threshold current predictions are incorrect by factors of up to 3 or 4, there will still be evidence of the beam breakup instability developing below 10 mA. Current efforts are focused on developing methods to suppress the onset of beam breakup.

Frequency (MHz)	**Loaded Q**	**(R/Q) (Ω)**	**Threshold Current (mA)**	**Orientation**	**Location**
2102.607	2.61×10^6	29.90	7.07	x-axis	Cavity 8
2104.683	1.94×10^6	29.90	7.86	x-axis	Cavity 5
2106.007	6.11×10^6	29.90	2.85	y-axis	Cavity 7
2114.156	5.21×10^6	28.80	3.68	x-axis	Cavity 4
2115.201	2.17×10^6	28.80	8.28	y-axis	Cavity 6
2116.055	3.06×10^6	28.80	4.99	x-axis	Cavity 1
2116.585	6.66×10^6	28.80	4.18	x-axis	Cavity 7

Table 3: Summary of the MATBBU simulation showing mode properties of those HOMs which are predicted to produce threshold currents below 10 mA.

Appendix A: Setup for Measuring HOMs in the 7-Cell Cryomodule

The loaded Qs of the higher-order modes were measured in the following way:

We excite a cavity through the fundamental power coupler (via the waveguide and a top hat) using port 1 of the network analyzer. The top hat is used to provide the proper impedance match from the waveguide to a 50 Ω coaxial cable. Port 2 of the network analyzer is connected to the HOM1 port while the field probe and HOM2 ports are terminated in 50 Ω loads. This completes the S21 measurement. From the resulting spectra the frequencies of the HOMs can be read off. The loaded quality-factor of each mode is found from the center frequency divided by the bandwidth between the -3 dB points.

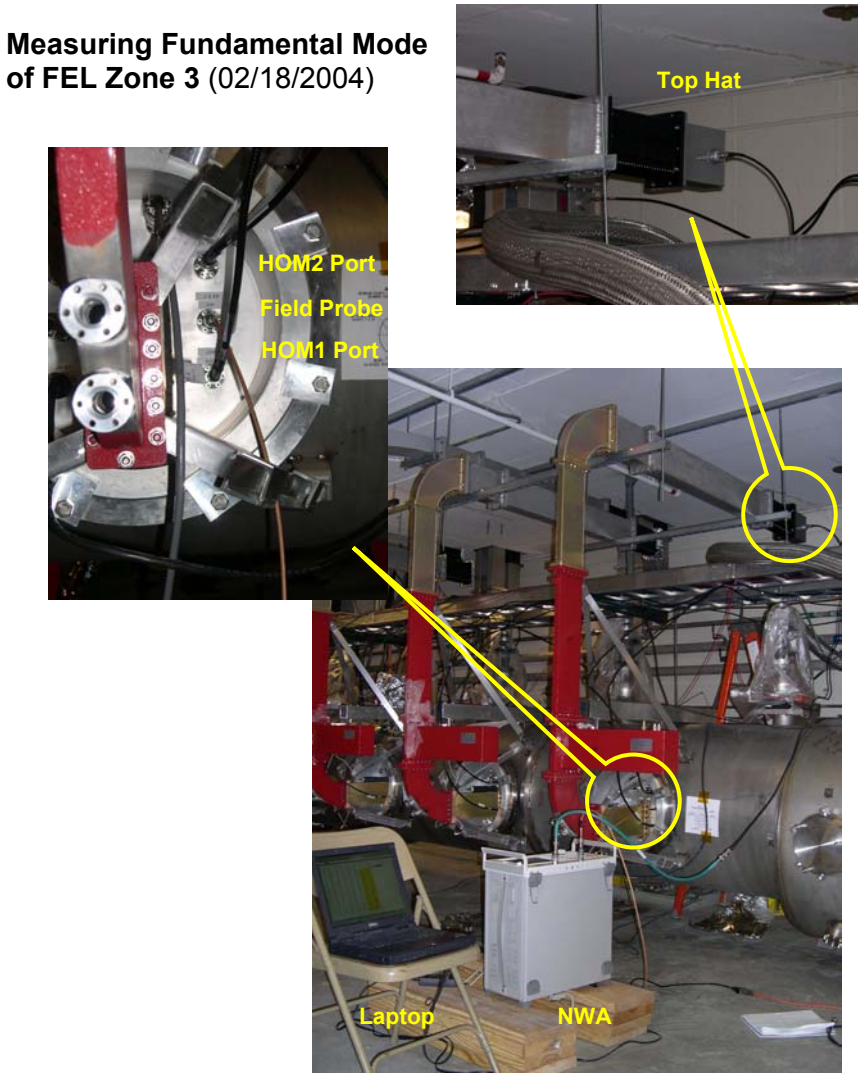

Appendix B: $(R/Q)Q_L$ for the HOMs in the First Two Passbands in Each Cavity (courtesy H. Wang [10])

Note: *The shunt impedance is in MAFIA units of {Ω/cm^2}. For the TDBBU input file, the shunt impedance must be normalized and be in units of {Ω}.*

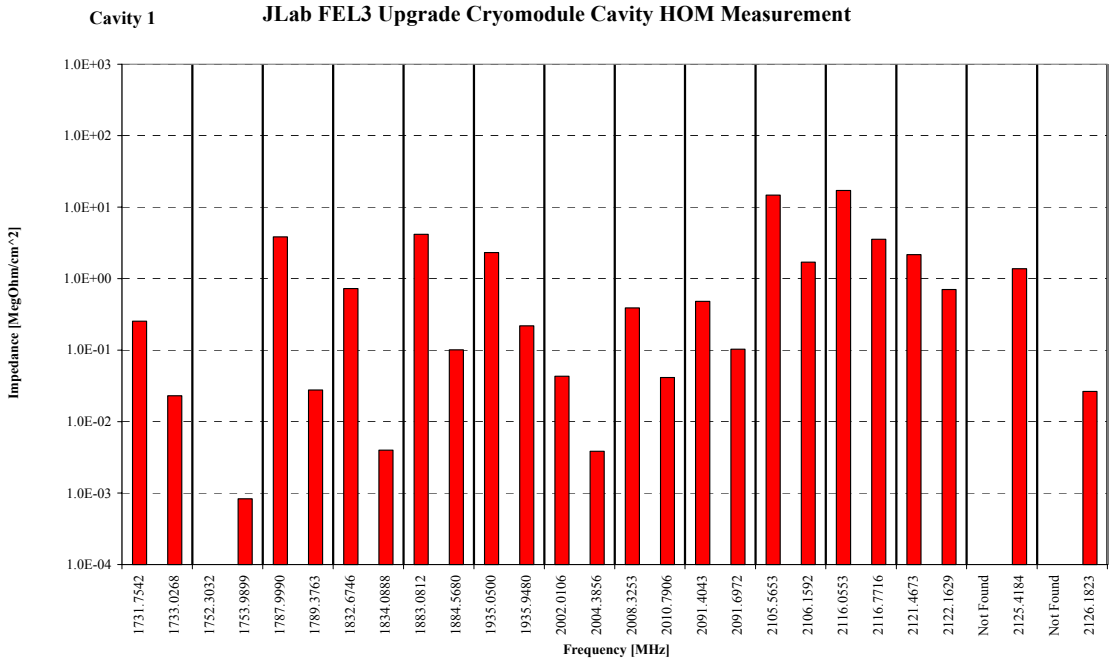

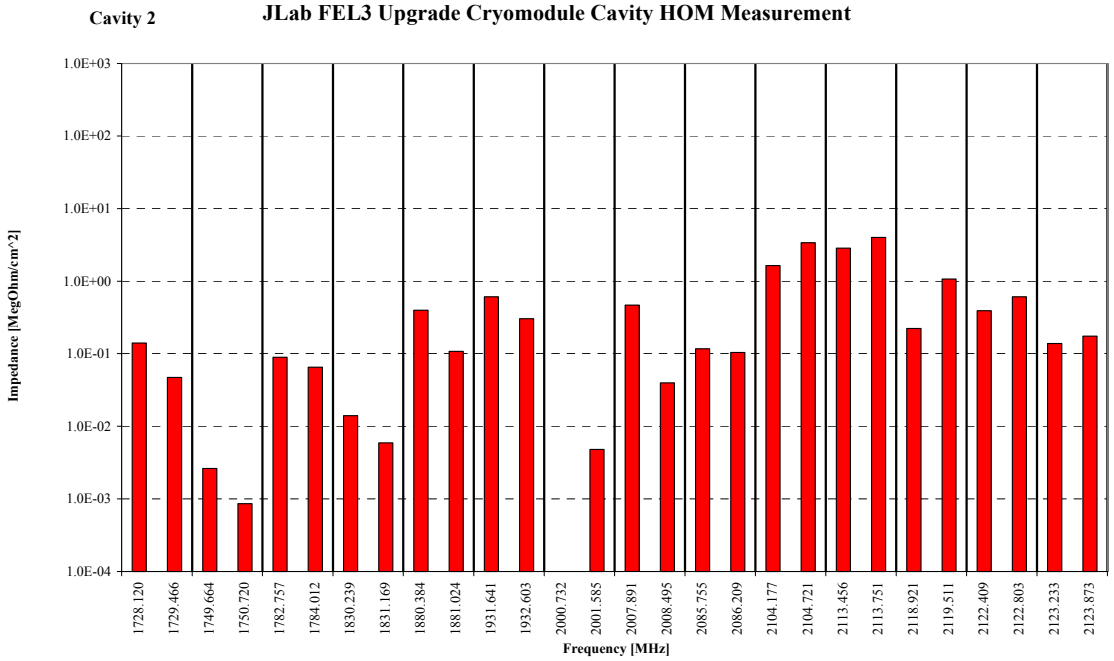

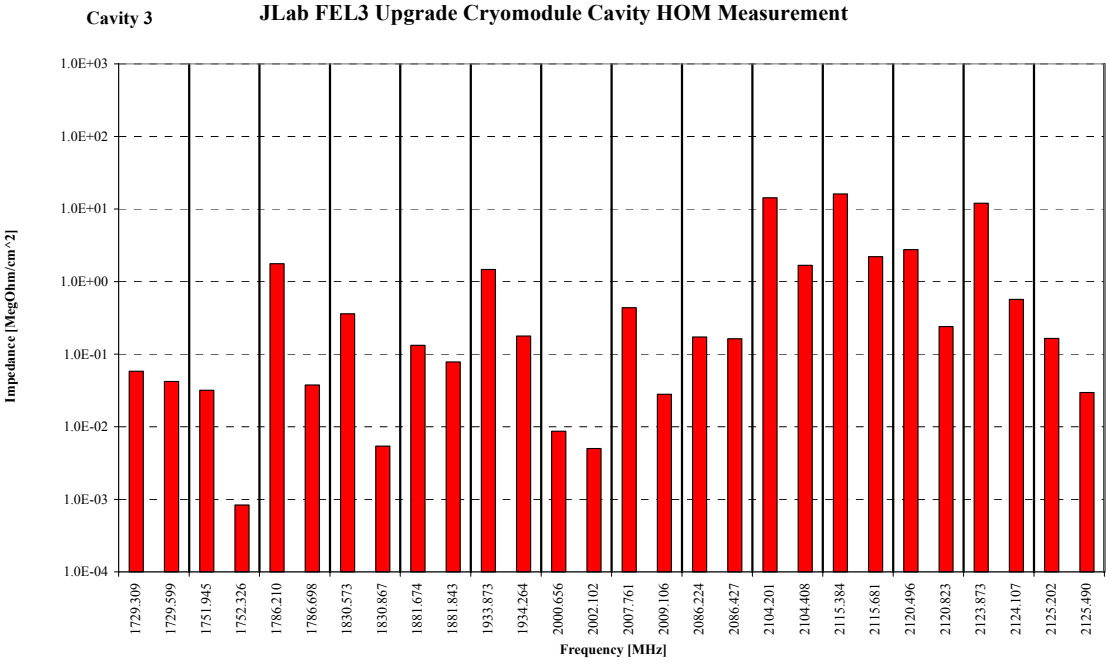
Cavity 3
JLab FEL3 Upgrade Cryomodule Cavity HOM Measurement
Impedance [MegOhm/cm^2]
1.0E+03
1.0E+02
1.0E+01
1.0E+00
1.0E-01
1.0E-02
1.0E-03
1.0E-04
1729.309
1729.599
1751.945
1752.326
1786.210
1786.698
1830.573
1830.867
1881.674
1881.843
1933.873
1934.264
2000.656
2002.102
2007.761
2009.106
2086.224
2086.427
2104.201
2104.408
2115.384
2115.681
2120.496
2120.823
2123.873
2124.107
2125.202
2125.490
Frequency [MHz]

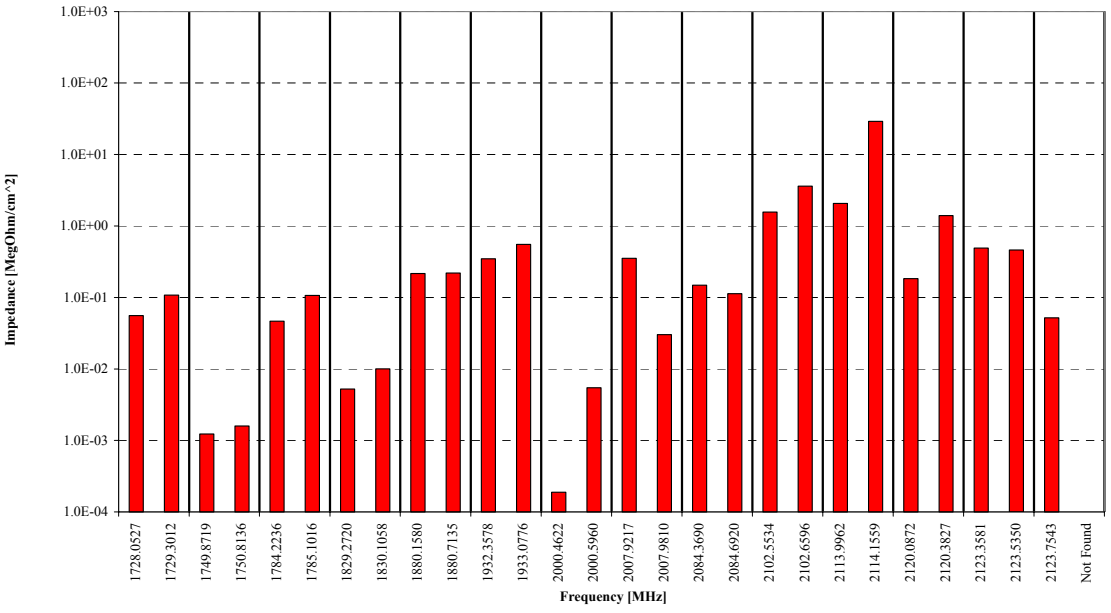
Cavity 4
JLab FEL3 Upgrade Cryomodule Cavity HOM Measurement
Impedance [MegOhm/cm^2]
1.0E+03
1.0E+02
1.0E+01
1.0E+00
1.0E-01
1.0E-02
1.0E-03
1.0E-04
1728.0527
1729.3012
1749.8719
1750.8136
1784.2236
1785.1016
1829.2720
1830.1058
1880.1580
1880.7135
1932.3578
1933.0776
2000.4622
2000.5960
2007.9217
2007.9810
2084.3690
2084.6920
2102.5534
2102.6596
2113.9962
2114.1559
2120.0872
2120.3827
2123.3581
2123.5350
2123.7543
Not Found
Frequency [MHz]

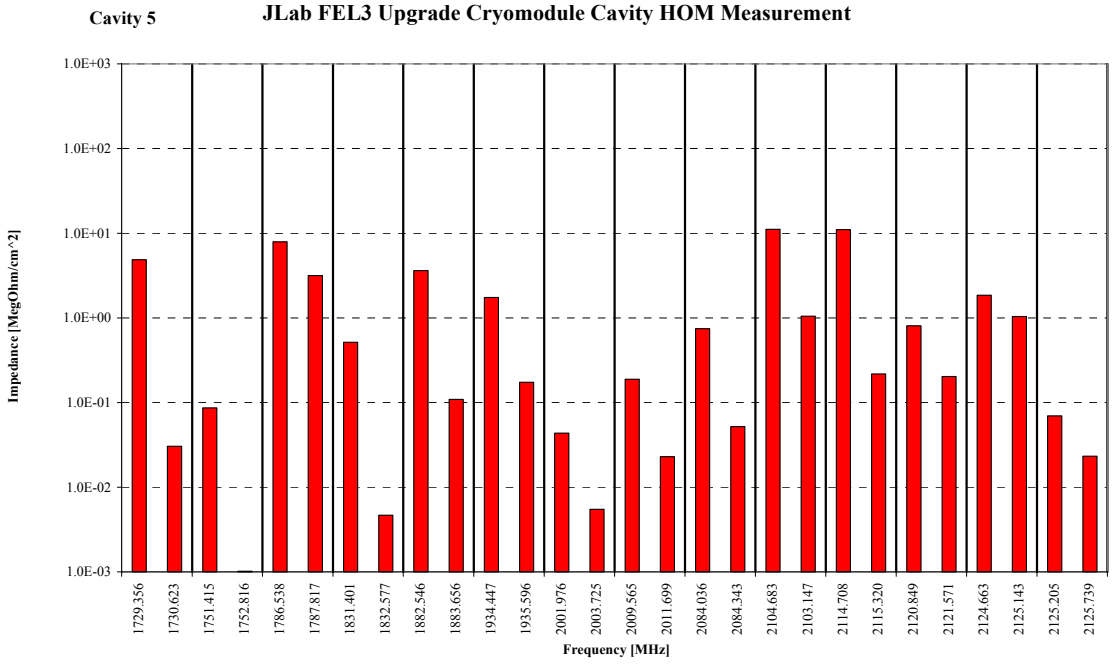
Cavity 5
JLab FEL3 Upgrade Cryomodule Cavity HOM Measurement
Impedance [MegOhm/cm^2]
1.0E+03
1.0E+02
1.0E+01
1.0E+00
1.0E-01
1.0E-02
1.0E-03
1729.356
1730.623
1751.415
1752.816
1786.538
1787.817
1831.401
1832.577
1882.546
1883.656
1934.447
1935.596
2001.976
2003.725
2009.565
2011.699
2084.036
2084.343
2104.683
2103.147
2114.708
2115.320
2120.849
2121.571
2124.663
2125.143
2125.205
2125.739
Frequency [MHz]

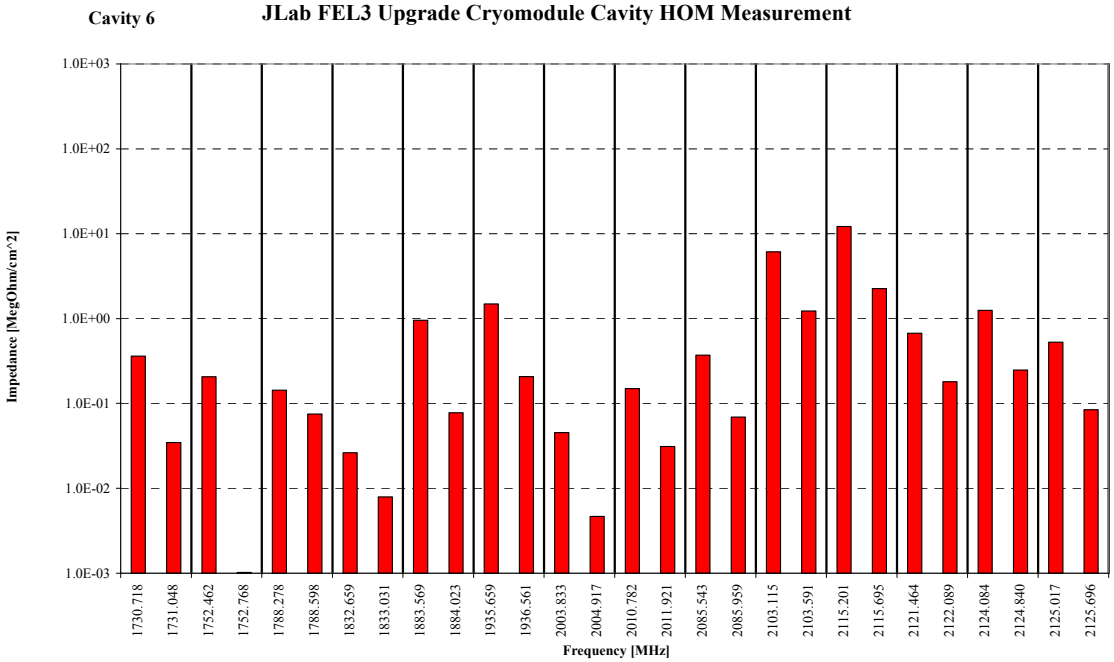
Cavity 6
JLab FEL3 Upgrade Cryomodule Cavity HOM Measurement
Impedance [MegOhm/cm^2]
1.0E+03
1.0E+02
1.0E+01
1.0E+00
1.0E-01
1.0E-02
1.0E-03
1730.718
1731.048
1752.462
1752.768
1788.278
1788.598
1832.659
1833.031
1883.569
1884.023
1935.659
1936.561
2003.833
2004.917
2010.782
2011.921
2085.543
2085.959
2103.115
2103.591
2115.201
2115.695
2121.464
2122.089
2124.084
2124.840
2125.017
2125.696
Frequency [MHz]

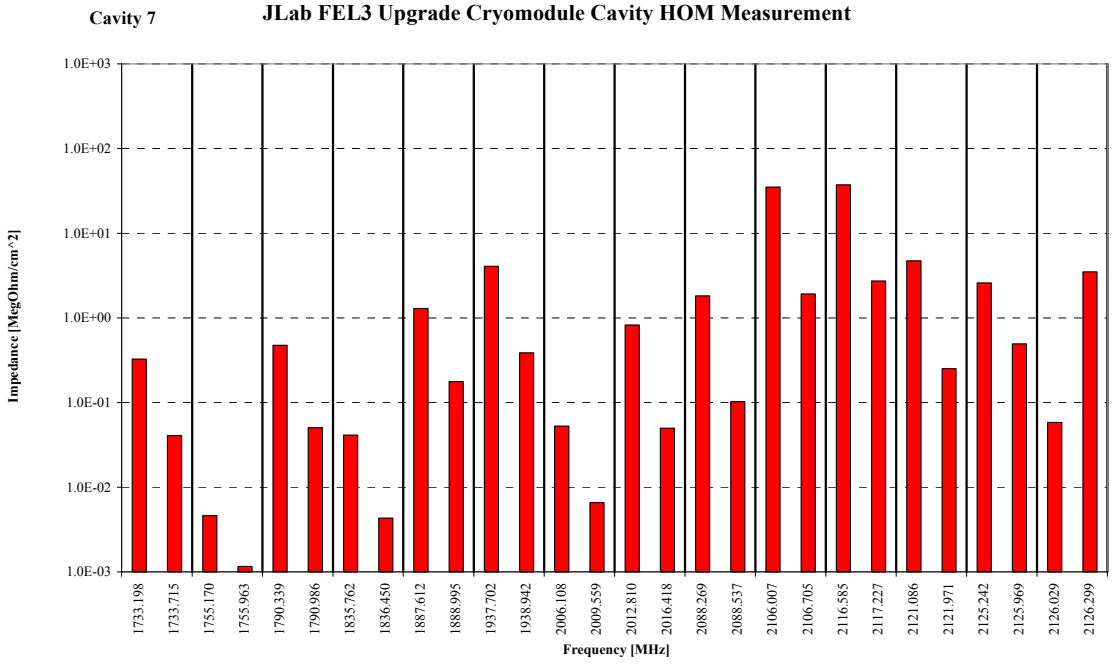
Cavity 7
JLab FEL3 Upgrade Cryomodule Cavity HOM Measurement
Impedance [MegOhm/cm^2]
1.0E+03
1.0E+02
1.0E+01
1.0E+00
1.0E-01
1.0E-02
1.0E-03
1733.198
1733.715
1755.170
1755.963
1790.339
1790.986
1835.762
1836.450
1887.612
1888.995
1937.702
1938.942
2006.108
2009.559
2012.810
2016.418
2088.269
2088.537
2106.007
2106.705
2116.585
2117.227
2121.086
2121.971
2125.242
2125.969
2126.029
2126.299
Frequency [MHz]

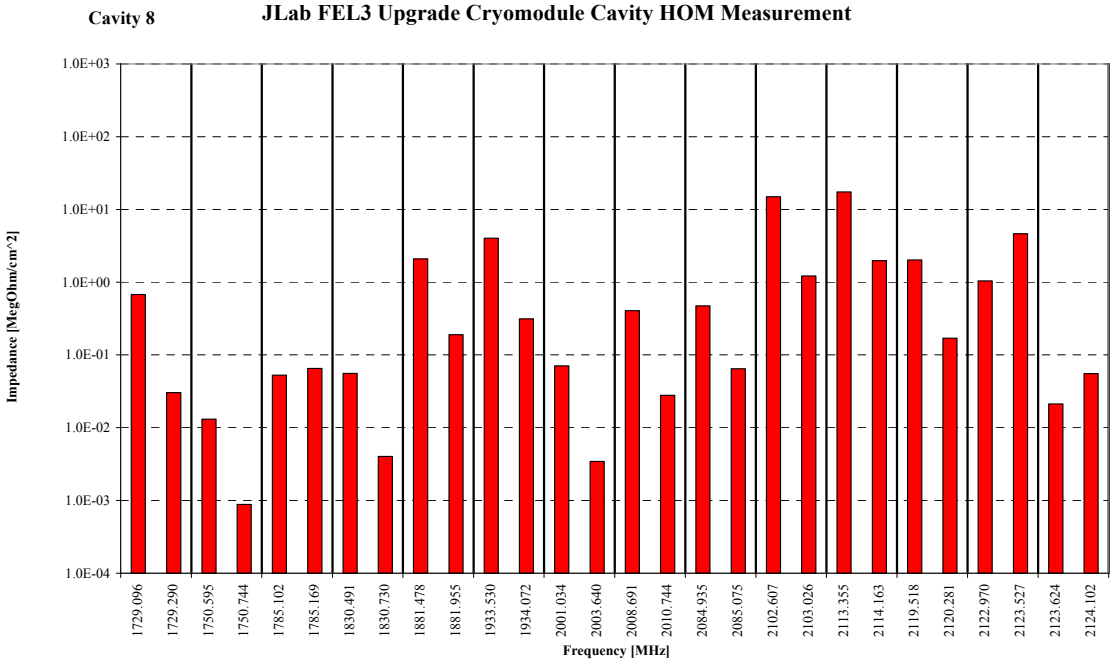
Cavity 8
JLab FEL3 Upgrade Cryomodule Cavity HOM Measurement
Impedance [MegOhm/cm^2]
1.0E+03
1.0E+02
1.0E+01
1.0E+00
1.0E-01
1.0E-02
1.0E-03
1.0E-04
1729.096
1729.290
1750.595
1750.744
1785.102
1785.169
1830.491
1830.730
1881.478
1881.955
1933.530
1934.072
2001.034
2003.640
2008.691
2010.744
2084.935
2085.075
2102.607
2103.026
2113.355
2114.163
2119.518
2120.281
2122.970
2123.527
2123.624
2124.102
Frequency [MHz]

Appendix C: MATBBU Input File

```
1TITLE 10kW IR FEL 145 MeV, April 2004 3CMs [0,7,0] cells
 DATA
 APRTR    100000.   2.0
 REF      0.        1500.     1500.00   700.00    500.0     0.0
 BEAM     10.0      2994.0    20.0      0.0       1.0       0.0
 XPRNT    2.0       203.0     1.0
 YPRNT    2.0       203.0     1.0
#CMPNT      4400.0   0.0       0.0       0.0       0.0       0.0
>DRIFT  1.100.0     0.0
1DRIFT  1. 53.41    0.0
1CECAV  1. 0.0      0.0
1DRIFT  1. 5.       0.0
1CECAV  1. 0.0      0.0
1DRIFT  1. 46.06    0.0
1CECAV  1. 0.0      0.0
1DRIFT  1. 5.       0.0
1CECAV  1. 0.0      0.0
1DRIFT  1. 46.06    0.0
1CECAV  1. 0.0      0.0
1DRIFT  1. 5.       0.0
1CECAV  1. 0.0      0.0
1DRIFT  1. 46.06    0.0
1CECAV  1. 0.0      0.0
1DRIFT  1. 5.       0.0
1CECAV  1. 0.0      0.0
1DRIFT  1. 53.41    0.0
1DRIFT  1. 85.1     0.0
1LENS   1.-3.597509 15.0
1DRIFT  1. 37.4     0.0
1LENS   1. 6.755323 15.0
1DRIFT  1. 37.4     0.0
1LENS   1.-3.597509 15.0
1DRIFT  1. 65.1     0.0
1DRIFT  1. 53.41    0.0
1CECAV  1. 0.0      0.0
1CAVITY    29.90    2610000.  2102.607  90.0
1CAVITY    29.90    2610000.  2102.607  .0
1CAVITY    28.80    3100000.  2113.355  90.0
1CAVITY    28.80    3100000.  2113.355  .0
1DRIFT  1. 5.       0.0
1CECAV  1. 0.0      0.0
1CAVITY    29.90    6110000.  2106.007  90.0
1CAVITY    29.90    6110000.  2106.007  .0
1CAVITY    28.80    6660000.  2116.585  90.0
1CAVITY    28.80    6660000.  2116.585  .0
1DRIFT  1. 46.06    0.0
1CECAV  1. 0.0      0.0
1CAVITY    28.80    2170000.  2115.201  90.0
1CAVITY    28.80    2170000.  2115.201  .0
1DRIFT  1. 5.       0.0
1CECAV  1. 0.0      0.0
1CAVITY    29.90    1940000.  2104.683  90.0
1CAVITY    29.90    1940000.  2104.683  .0
1CAVITY    28.80    1970000.  2114.708  90.0
1CAVITY    28.80    1970000.  2114.708  .0
1DRIFT  1. 46.06    0.0
1CECAV  1. 0.0      0.0
1CAVITY    28.80    5210000.  2114.156  90.0
1CAVITY    28.80    5210000.  2114.156  .0
1DRIFT  1. 5.       0.0
1CECAV  1. 0.0      0.0
1CAVITY    29.90    2490000.  2104.201  90.0
1CAVITY    29.90    2490000.  2104.201  .0
1CAVITY    28.80    2880000.  2115.384  90.0
1CAVITY    28.80    2880000.  2115.384  .0
1CAVITY    05.20    11900000. 2123.873  90.0
1CAVITY    05.20    11900000. 2123.873  .0
1DRIFT  1. 46.06    0.0
```

```
1CECAV  1. 0.0      0.0
1DRIFT  1. 5.       0.0
1CECAV  1. 0.0      0.0
1CAVITY    29.90    2570000.  2105.565  90.0
1CAVITY    29.90    2570000.  2105.565  .0
1CAVITY    28.80    3060000.  2116.055  90.0
1CAVITY    28.80    3060000.  2116.055  .0
1DRIFT  1. 53.41    0.0
2DRIFT  1. 65.1     0.0
2LENS   1. 1.294342 15.0
2DRIFT  1. 37.4     0.0
2LENS   1.-2.550615 15.0
2DRIFT  1. 37.4     0.0
2LENS   1. 1.294342 15.0
2DRIFT  1. 85.1     0.0
1DRIFT  1. 53.41    0.0
1CECAV  1. 0.0      0.0
1DRIFT  1. 5.       0.0
1CECAV  1. 0.0      0.0
1DRIFT  1. 46.06    0.0
1CECAV  1. 0.0      0.0
1DRIFT  1. 5.       0.0
1CECAV  1. 0.0      0.0
1DRIFT  1. 46.06    0.0
1CECAV  1. 0.0      0.0
1DRIFT  1. 5.       0.0
1CECAV  1. 0.0      0.0
1DRIFT  1. 46.06    0.0
1CECAV  1. 0.0      0.0
1DRIFT  1. 5.       0.0
1CECAV  1. 0.0      0.0
1DRIFT  1. 53.41    0.0
2DRIFT  1.100.0     0.0
$RECIRC 1.
$CALC     0.
0.1,0.,0,0.0,0.,0
0.1,0.,0,0.0,0.,0
1203
0.443548  -18.14799    0.0 0.0
0.0410076  0.576699    0.0 0.0
0.0 0.0   -1.152552    17.68565
0.0 0.0    0.03581095  -1.417150
0.0,0.,0,0.,0.,0
0.0,0.,0,0.,0.,0
```

CAVMAT File

The cavmat (*cav*ity *mat*rix) file for the FEL Upgrade is given below. Each row contains the energy change {MeV} due to a single cavity, the length of the cavity {cm} and the 4 x 4 transverse transfer matrix (M_{11}, M_{12}, M_{21}, M_{22}, M_{33}, M_{34}, M_{43}, M_{44}). Note that for energy recovery, the change in energy is negative to indicate deceleration.

```
! ZONE 2 ACCELERATION
5.075790532000000   70.  0.778246  0.561123  -0.101322  0.783395  0.778246  0.561123  -0.101322  0.783395
5.075790532000000   70.  0.846077  0.600681  -0.054275  0.847917  0.846077  0.600681  -0.054275  0.847917
5.075790532000000   70.  0.882194  0.622667  -0.033786  0.883019  0.882194  0.622667  -0.033786  0.883019
5.075790532000000   70.  0.904606  0.636675  -0.023047  0.905029  0.904606  0.636675  -0.023047  0.905029
5.075790532000000   70.  0.919863  0.646383  -0.016723  0.920100  0.919863  0.646383  -0.016723  0.920100
5.075790532000000   70.  0.930917  0.653509  -0.012686  0.931057  0.930917  0.653509  -0.012686  0.931057
5.075790532000000   70.  0.939294  0.658962  -0.009953  0.939380  0.939294  0.658962  -0.009953  0.939380
5.075790532000000   70.  0.945860  0.663270  -0.008017  0.945915  0.945860  0.663270  -0.008017  0.945915
! ZONE 3 ACCELERATION
6.980883460000000   70.  0.933387  0.655120  -0.011875  0.933524  0.933387  0.655120  -0.011875  0.933524
6.980883460000000   70.  0.941211  0.660223  -0.009386  0.941297  0.941211  0.660223  -0.009386  0.941297
6.980883460000000   70.  0.947391  0.664283  -0.007605  0.947447  0.947391  0.664283  -0.007605  0.947447
6.980883460000000   70.  0.952396  0.667591  -0.006287  0.952433  0.952396  0.667591  -0.006287  0.952433
6.980883460000000   70.  0.956532  0.670338  -0.005284  0.956556  0.956532  0.670338  -0.005284  0.956556
6.980883460000000   70.  0.960007  0.672656  -0.004504  0.960023  0.960007  0.672656  -0.004504  0.960023
6.980883460000000   70.  0.962968  0.674637  -0.003884  0.962978  0.962968  0.674637  -0.003884  0.962978
6.980883460000000   70.  0.965521  0.676351  -0.003384  0.965527  0.965521  0.676351  -0.003384  0.965527
! ZONE 4 ACCELERATION
5.077089683000000   70.  0.976445  0.683742  -0.001613  0.976442  0.976445  0.683742  -0.001613  0.976442
5.077089683000000   70.  0.977505  0.684463  -0.001474  0.977502  0.977505  0.684463  -0.001474  0.977502
5.077089683000000   70.  0.978473  0.685124  -0.001353  0.978470  0.978473  0.685124  -0.001353  0.978470
5.077089683000000   70.  0.979362  0.685730  -0.001246  0.979358  0.979362  0.685730  -0.001246  0.979358
5.077089683000000   70.  0.980180  0.686289  -0.001151  0.980176  0.980180  0.686289  -0.001151  0.980176
5.077089683000000   70.  0.980935  0.686806  -0.001066  0.980932  0.980935  0.686806  -0.001066  0.980932
5.077089683000000   70.  0.981635  0.687286  -0.000991  0.981632  0.981635  0.687286  -0.000991  0.981632
5.077089683000000   70.  0.982286  0.687731  -0.000923  0.982283  0.982286  0.687731  -0.000923  0.982283
! ZONE 2 DECELERATION
-5.07579053200000   70.  1.017367  0.712290  -0.000958  1.017354  1.017367  0.712290  -0.000958  1.017354
-5.07579053200000   70.  1.017992  0.712737  -0.001029  1.017977  1.017992  0.712737  -0.001029  1.017977
-5.07579053200000   70.  1.018664  0.713218  -0.001109  1.018647  1.018664  0.713218  -0.001109  1.018647
-5.07579053200000   70.  1.019387  0.713737  -0.001199  1.019369  1.019387  0.713737  -0.001199  1.019369
-5.07579053200000   70.  1.020169  0.714298  -0.001300  1.020149  1.020169  0.714298  -0.001300  1.020149
-5.07579053200000   70.  1.021017  0.714907  -0.001414  1.020995  1.021017  0.714907  -0.001414  1.020995
-5.07579053200000   70.  1.021939  0.715570  -0.001544  1.021915  1.021939  0.715570  -0.001544  1.021915
-5.07579053200000   70.  1.022945  0.716295  -0.001693  1.022918  1.022945  0.716295  -0.001693  1.022918
! ZONE 3 DECELERATION
-6.98088346000000   70.  1.033202  0.723736  -0.003626  1.033130  1.033202  0.723736  -0.003626  1.033130
-6.98088346000000   70.  1.035562  0.725463  -0.004182  1.035475  1.035562  0.725463  -0.004182  1.035475
-6.98088346000000   70.  1.038283  0.727461  -0.004877  1.038178  1.038283  0.727461  -0.004877  1.038178
-6.98088346000000   70.  1.041455  0.729799  -0.005762  1.041324  1.041455  0.729799  -0.005762  1.041324
-6.98088346000000   70.  1.045199  0.732572  -0.006910  1.045034  1.045199  0.732572  -0.006910  1.045034
-6.98088346000000   70.  1.049686  0.735915  -0.008440  1.049471  1.049686  0.735915  -0.008440  1.049471
-6.98088346000000   70.  1.055159  0.740023  -0.010541  1.054871  1.055159  0.740023  -0.010541  1.054871
-6.98088346000000   70.  1.061985  0.745191  -0.013538  1.061583  1.061985  0.745191  -0.013538  1.061583
! ZONE 4 DECELERATION
-5.07708968300000   70.  1.051058  0.736947  -0.008961  1.050834  1.051058  0.736947  -0.008961  1.050834
-5.07708968300000   70.  1.056855  0.741309  -0.011272  1.056551  1.056855  0.741309  -0.011272  1.056551
-5.07708968300000   70.  1.064131  0.746837  -0.014608  1.063703  1.064131  0.746837  -0.014608  1.063703
-5.07708968300000   70.  1.073536  0.754075  -0.019680  1.072897  1.073536  0.754075  -0.019680  1.072897
-5.07708968300000   70.  1.086155  0.763960  -0.027942  1.085128  1.086155  0.763960  -0.027942  1.085128
-5.07708968300000   70.  1.103951  0.778266  -0.042765  1.102116  1.103951  0.778266  -0.042765  1.102116
-5.07708968300000   70.  1.130848  0.800813  -0.073540  1.126976  1.130848  0.800813  -0.073540  1.126976
-5.07708968300000   70.  1.175684  0.841568  -0.155449  1.164771  1.175684  0.841568  -0.155449  1.164771
```

Appendix D: Active HOM Damping Scheme

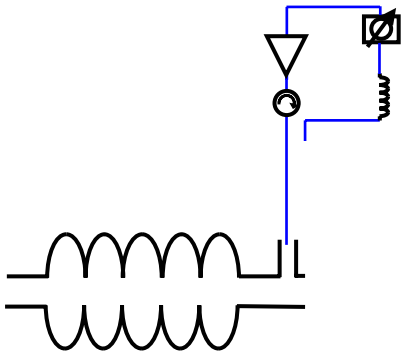

Schematic of the HOM damping setup. We used a variable attenuator to control the gain of the loop. We coupled power from the HOM1 port and then fed the power back, 180 degrees out of phase, through the HOM2 port.

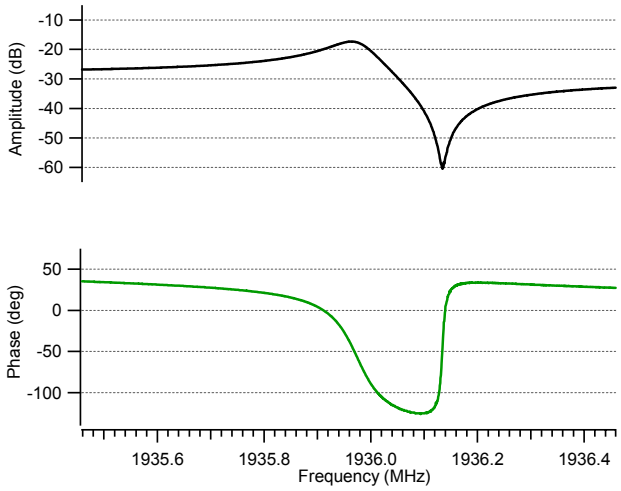

Resonance curve and phase plot of HOM at 1936 MHz *before* active damping.

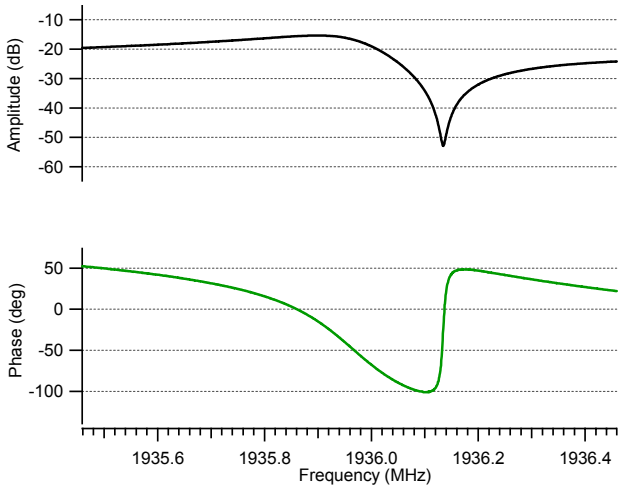

Resonance curve and phase plot of HOM at 1936 MHz *after* active damping. Notice the broadening of the resonance curve and the corresponding change in the phase plot. This results in a lower loaded Q. (From the data the Q has been damped by a factor of ~ 4).

References

[1] Bisognano, J., Gluckstern, R., "Multipass Beam Breakup in Recirculating Linacs", Proceedings of the Particle Accelerator Conference (1987).

[2] Sereno, N., "Experimental Studies of Multipass Beam Breakup and Energy Recovery Using the CEBAF Injector Linac", Ph.D Thesis, U. of Illinois at Urbana-Champaign (1994).

[3] Wang, H., et. al., "HOM Damping Performance of the JLab SL21 Cryomodule", Proceedings of the Particle Accelerator Conference (2003).

[4] *Tennant, unpublished* (2003).

[5] Beard, K., et. al., "Estimates of the Beam Breakup Thresholds in the 10 kW FEL due to HOMs", JLAB-TN-02-042 (2002).

[6] Yunn, B., "Dipole Mode HOM Damping Requirements of the New 7-Cell Cavity for the 12 GeV CEBAF Upgrade", JLAB-TN-01-028 (2001).

[7] D. Douglas, *private communication*.

[8] R. Rimmer, *private communication*.

[9] Tennant, C., "Modeling a Transverse Feedback System for an Energy Recovery Linac", JLAB-TN-03-045 (2003).

[10] Wang, H., Microsoft Excel Spreadsheet (2004).